

Sarcolemma phospholipid structure investigated by immunogold electron microscopy and ^{31}P NMR spectroscopy with lanthanide ions

Céline Moreau^{a,*}, Annie Cavalier^b, Marie Le Floch^c, Jacqueline Segalen^a, Chantal Rocher^a, Mounir Traïkia^a, Geneviève Leray^a, Arnaud Bondon^d, Daniel Thomas^b, Elisabeth Le Rumeur^a

^aLaboratoire de RMN en Biologie et Médecine (LRMBM-UPRES 2230), Faculté de Médecine, CS 34317, 35043 Rennes Cedex, France

^bCanaux et récepteurs membranaires, UMR CNRS 6026, Université de Rennes 1, Campus de Beaulieu, 35042 Rennes Cedex, France

^cVerres et Céramiques, UMR CNRS 6512, Université de Rennes 1, Campus de Beaulieu, 35042 Rennes Cedex, France

^dLaboratoire de Chimie Organométallique et Biologique, UMR CNRS 6509, Université de Rennes 1, Campus de Beaulieu, 35042 Rennes Cedex, France

Received 17 October 2001; accepted 13 November 2001

First published online 23 November 2001

Edited by Felix Wieland

Abstract The biological functions of plasma membranes depend greatly on the biophysical properties resulting from protein and phospholipid structure. We investigated the phospholipid structure of the normal sarcolemma membrane, which is known to be highly dysfunctional in myopathies. Combining electron microscopy and ^{31}P nuclear magnetic resonance (NMR) spectroscopy on isolated sarcolemma vesicles, we find that (i) the sarcolemma vesicles maintain the in-vivo cellular sidedness, (ii) the phospholipid mobility is close to that observed in model membranes (similar lateral diffusion coefficients and spin-lattice T_1 relaxation times). Using broad-band and magic angle spinning ^{31}P NMR spectroscopy with lanthanide ions (Pr^{3+}), it is possible to quantify the distribution of phospholipids between internal and external membrane layers, showing that the trans-bilayer distribution is highly asymmetrical. © 2001 Federation of European Biochemical Societies. Published by Elsevier Science B.V. All rights reserved.

Key words: Phospholipid trans-bilayer distribution; Lanthanide ion; Magic angle spinning nuclear magnetic resonance; Vesicle sidedness

1. Introduction

Profound dysfunction and disruption of the plasma membrane occur in the skeletal muscle of subjects with myopathy due to a disease process affecting the protein composition of skeletal muscle sarcolemma or subsarcolemma [1,2]. Although protein–protein interactions have been widely investigated in

the skeletal muscle plasma membrane, little is known about the phospholipid (PL) structure and particularly the trans-bilayer distribution.

As a rule, all eukaryotic cells are now thought to exhibit an asymmetrical trans-bilayer distribution of lipids [3–6]. This lipid topology was first demonstrated in the human erythrocyte plasma membrane and later in several other types of cell; it appears to be essential for maintaining membrane properties and functions [7–9]. A range of indirect methods has been used to determine the lipid distribution in these natural membranes [10–12].

In the case of model membranes such as liposomes, a very popular and widely developed strategy is to use paramagnetic chemical shift reagents and nuclear magnetic resonance (NMR) spectroscopy [13–23]. The distribution of PLs between the two layers of the model membrane has been investigated with NMR spectroscopy using Pr^{3+} , Dy^{3+} and Eu^{3+} paramagnetic ions. These lanthanide ions induce a chemical shift and/or a broadening of NMR lines, but they do not penetrate into the membrane [16–18,21–23]. Apart from one report [24], this strategy has only been performed on the type of model membrane that yields high-resolution ^{31}P NMR spectra, i.e. small unilamellar vesicles (SUVs). In other model membranes such as multilamellar vesicles, membrane lipids undergo a slow isotropic motion on the NMR time scale. As this motion cannot average the chemical shift anisotropy (CSA) of the phosphorus nuclei, unresolved powder-like ^{31}P NMR spectrum appear. The same applies for subcellular preparations of sealed vesicles.

Magic angle spinning (MAS) NMR spectroscopy offers new possibilities for investigating membrane structure because it can overcome the problem of unresolved spectra. This is done by averaging the CSA, yielding narrow lines [25–27] that are relatively easy to analyse and quantify [28,29].

In a previous study, we have shown that MAS ^{31}P NMR spectroscopy can identify the PLs in sarcolemma vesicles isolated from normal rabbit skeletal muscle [30]. In order to characterise the arrangement of sarcolemma PLs in more detail, we now apply a strategy combining electron microscopy and ^{31}P NMR spectroscopy with lanthanide ions. In a first step, electron microscopy allows us to check vesicle formation and membrane sidedness. Then, solid-state and MAS ^{31}P NMR spectroscopy using lanthanide ions provides informa-

*Corresponding author. Fax: (33)-2-336892.

E-mail addresses: celine.moreau@univ-rennes1.fr (C. Moreau), annie.cavalier@univ-rennes1.fr (A. Cavalier), marie.lefloch@univ-rennes1.fr (M. Le Floch), jacqueline.segalen@univ-rennes1.fr (J. Segalen), chantal.rocher@univ-rennes1.fr (C. Rocher), mounir.traïkia@free.fr (M. Traïkia), genevieve.leray@univ-rennes1.fr (G. Leray), arnaud.bondon@univ-rennes1.fr (A. Bondon), daniel.thomas@univ-rennes1.fr (D. Thomas), elisabeth.lerumeur@univ-rennes1.fr (E. Le Rumeur).

Abbreviations: MAS, magic angle spinning; CSA, chemical shift anisotropy; PL, phospholipid

tion about the trans-bilayer distribution of the membrane PLs.

2. Materials and methods

2.1. Sarcolemma membranes

Sarcolemma membranes from New Zealand white rabbit skeletal muscle (CEGAV Society, France) were isolated as previously described [30,34]. Briefly, the skeletal muscle was homogenised in buffer A (20 mM sodium pyrophosphate, 20 mM sodium phosphate, 1 mM MgCl_2 , 0.303 M sucrose, 0.5 mM EDTA, pH 7.0 and protease inhibitors). The homogenate was subjected to differential centrifugation steps and the resultant light microsomes were then loaded onto a sucrose gradient and centrifuged at $104\,000 \times g$ for 17 h at 4°C. The final preparation was obtained in buffer B (0.303 M sucrose, 20 mM Tris-maleate, pH 7.0, and protease inhibitors), corresponding to a protein concentration of about 50 mg/ml.

2.2. Transmission electron microscopy

2.2.1. Ultrathin sections. Sarcolemma vesicles were visualised as previously described [30]. To summarize, ultrathin sections were cut from embedded pellets of vesicles, stained with uranyl acetate and lead citrate, and then observed under a JEOL electron microscope (JEOL Europe, SA) operating at 80 kV.

The diameter of the vesicles was measured manually on micrographs having the same magnification of samples with or without PrCl_3 . To some extent, the diameter seems to be preparation dependent and values are expressed in the text as ranges.

2.2.2. Immunolocalisation of dystrophin and α -dystroglycan. Freshly isolated sarcolemma vesicles (four different preparations) were deposited on collodion carbon-coated nickel grids and incubated in 1% bovine serum albumin (BSA) in phosphate-buffered saline (PBS) for 2 h at room temperature. Vesicles were then incubated for 2 h with primary monoclonal mouse anti-dystrophin (1:100 dilution, Sigma) or anti- α -dystroglycan (1:500 dilution, Euromedex) antibodies, rinsed three times with PBS-BSA, and incubated for 1 h with a 10-nm GAM-gold secondary antibody (TEBU, France) diluted 40-fold in PBS-BSA. After washing, the grids were stained with 2% uranyl acetate and viewed using a Philips CM12 microscope operating at 100 kV [31].

2.3. ^{31}P NMR spectroscopy

Sarcolemma vesicles at a concentration of about 50 mg/ml protein were introduced into a 4-mm-diameter ceramic rotor with a volume of 100 μl . Alternatively, the paramagnetic agent PrCl_3 (0.5–10 mM) was added to the exterior of the membrane vesicle before introduction into the rotor. ^{31}P NMR spectra were obtained at 121.9 or 202.4 MHz in 4-mm MAS probes on ASX300 and DMX500 Bruker spectrometers, respectively (Bruker spectrosin, Wissembourg, France) at 25°C using a single 90° pulse sequence with 5 s repetition delay. Broad-band spectra without or with proton decoupling were acquired using 10 000 scans, 5 μs dwell-time, 100 kHz spectral width, 8 K data points and 41 ms acquisition time. At 8 kHz MAS, spectra were acquired with or without proton decoupling using 1000–4000 scans, 10 μs dwell-time, 50 kHz spectral width and 16 K data points.

T_1 longitudinal relaxation times were measured at 121.9 MHz at 25°C, with 8 kHz MAS rate, using a progressive saturation pulse sequence, for samples with or without PrCl_3 .

Before applying the Fourier transform, free induction decays were treated with an exponential broadening of 100 and 5 Hz for static and spinning samples, respectively. 85% H_3PO_4 was used as an external standard for the ^{31}P chemical shift.

2.4. ^{31}P NMR spectral simulation and quantification

Deconvolution and quantification of the broad-band static and high-resolution spectra (MAS NMR spectra) were performed by CSA and Lorentzian/Gaussian peak-shape fitting with WinFit Software (Bruker Spectrospin, Wissembourg, France) [30].

The simulation programme used for treating the broad-band static spectrum was developed [32] and modified [33] to include vesicle size distribution. The simulation procedure is described in detail in [33]. Here, we assume that an axially symmetric tensor represents the CSA of the phosphate component of PLs in biological membranes. This is due to the rapid motion of the PLs around the local normal of the

bilayer, with an effective CSA value of 45 ± 5 ppm. Hence, the effect of vesicle size distribution can be taken into account in ^{31}P NMR spectra simulations by incorporating additional averaging procedures: (i) the rotational diffusion of the vesicles, with a characteristic correlation time τ_r ; (ii) the lateral diffusion of PLs along the curved surfaces, with a characteristic correlation time τ_{diff} . We can introduce an effective characteristic time, defined by the following expression:

$$1/\tau = 1/\tau_r + 1/\tau_{\text{diff}} = D/r^2 (D_r + D_{\text{diff}})$$

where $D_r = kT/8\pi r\eta$ is the rotational diffusion coefficient of the vesicles, η is the viscosity of the medium and r the radius of the vesicle. In our simulation programme, the distribution of the radius values is represented by particular size-distribution profiles. The following values were used in the simulations: $T = 298$ K, $D_{\text{diff}} = 10^{-7}$ cm^2/s and $\eta = 7.808 \times 10^{-4}$ P [32,33].

3. Results

3.1. Electron microscopy of sarcolemma vesicles

Electron microscopy shows that PrCl_3 added at the exterior of the vesicles induces some vesicle aggregation, but no fusion is observed. Diameters of 200–250 nm and 230–290 nm are obtained without and with PrCl_3 , respectively (Fig. 1).

3.2. Do the vesicles maintain cellular sidedness?

After using the Western blot method to check for the presence of dystrophin (an intracellular subsarcolemma protein) or α -dystroglycan (an extracellular matrix protein) in the sarcolemma vesicles (data not shown), we carried out immuno-gold-labelling of each of these proteins in the vesicle membranes (Fig. 2). The presence of gold particles as dark spheres on the micrographs indirectly indicates labelling of the corresponding protein. On the micrographs obtained from immuno-labelling with α -dystroglycan, gold particles are observed on the periphery of vesicles, indicating that α -dystroglycan is present at the outer rim of these vesicles (Fig. 2A). On the contrary, no gold particles were observed on the micrographs obtained from immuno-labelling with dystrophin (Fig. 2B). This indicates that dystrophin is not present on the vesicle rims, but is rather located inside the vesicles.

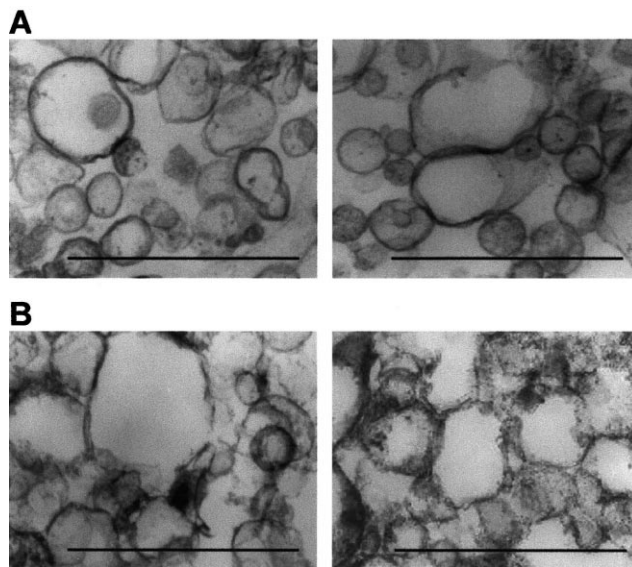


Fig. 1. Ultrathin electron microscopy sections of sarcolemma vesicles from (A) control preparations and (B) from preparations in contact with 5 mM PrCl_3 . Scale bar: 1 μm

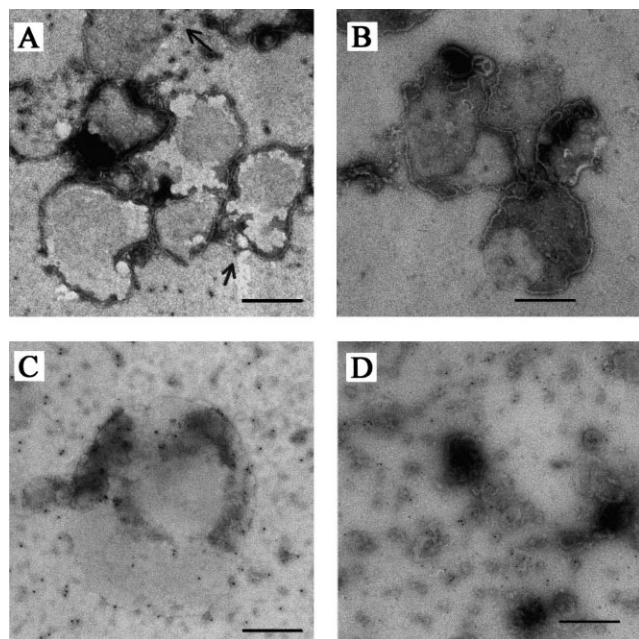


Fig. 2. Immunogold-labelling electron microscopy of (A,C) α -dystroglycan and (B,D) dystrophin in (A,B) intact and (B,D) sonicated sarcolemma vesicles (examples from four identical experiments). An arrow indicates the presence of a gold particle. Scale bar: 0.5 μ m.

Alternatively, dystrophin could be undetectable by immunogold labelling even if present. When immunogold labelling is performed on sonicated vesicles, gold particles are observed for both proteins in many of the fragments (Fig. 2C,D). This demonstrates that dystrophin is not located on the outer side but only on the inner side of intact sarcolemma vesicles. From these experiments, it appears that the vesicle membranes maintain cellular sidedness with dystrophin inside the vesicle and α -dystroglycan at the outer side.

3.3. Broad-band ^{31}P NMR spectra of sarcolemma vesicles

As previously observed, the experimental broad-band ^{31}P NMR spectrum of the sarcolemma vesicles is predominantly powder-like, characteristic of relatively large vesicles made up of PLs in a bilayer arrangement (Fig. 3) [30,33]. When comparing non-proton-decoupled (Fig. 3A) and proton-decoupled (Fig. 3B) spectra, the high-field peak is slightly better resolved with decoupling, but the CSA values are similar in both spectra (42 ppm). This experiment shows there is no drastic influence of the hetero-nuclear dipolar interaction on the line-shape of the spectrum at high field.

Two narrow resonances at 2 ppm and -7.1 ppm were assigned to phosphorus nuclei from inorganic phosphorus and sodium pyrophosphate, respectively, present in the homogenisation buffer A [30]. Small fluctuations of the amount of inorganic phosphorus and sodium pyrophosphate were observed in various preparations.

To simulate the spectrum, several types of size distribution were tested. Within each type of profile, we varied the parameters to fit experimental and simulated spectra by comparing the integrals of the spectra normalised to the same maximum intensity (Fig. 4) [33]. The best-simulated spectrum is obtained by assuming a Gaussian distribution of unilamellar vesicle size with an average diameter of 250 ± 70 nm, which is in the same range of size determined by electron microscopy. A good

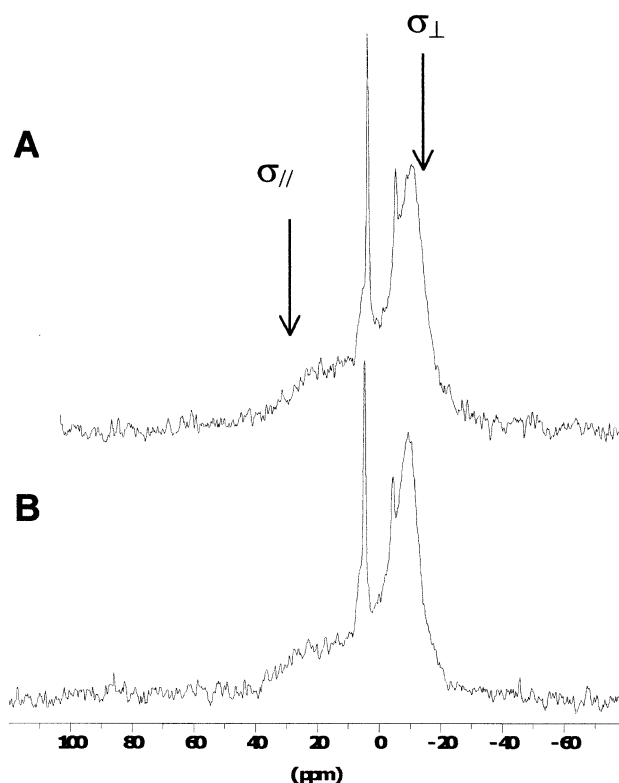


Fig. 3. (A) Experimental non-decoupled and (B) proton decoupled broad-band ^{31}P NMR spectra of sarcolemma vesicles performed at 202 MHz. σ_{\parallel} and σ_{\perp} are the chemical shift anisotropy tensors.

agreement was obtained between NMR and electron microscopy to determine vesicle mean diameters using $D_{\text{diff}} = 10^{-7}$ cm^2/s , a result which is consistent with the fluid state of the vesicle membrane.

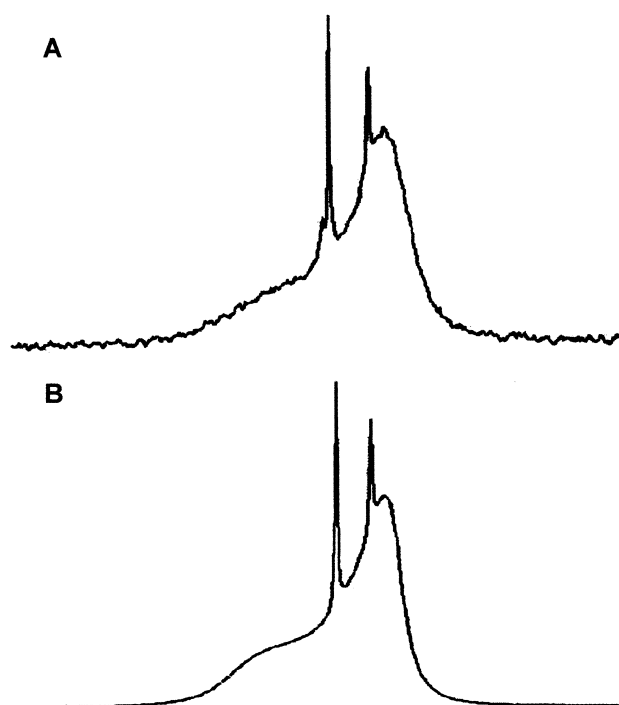


Fig. 4. (A) Experimental and (B) simulated broad-band ^{31}P NMR spectra of sarcolemma vesicles performed at 121 MHz.

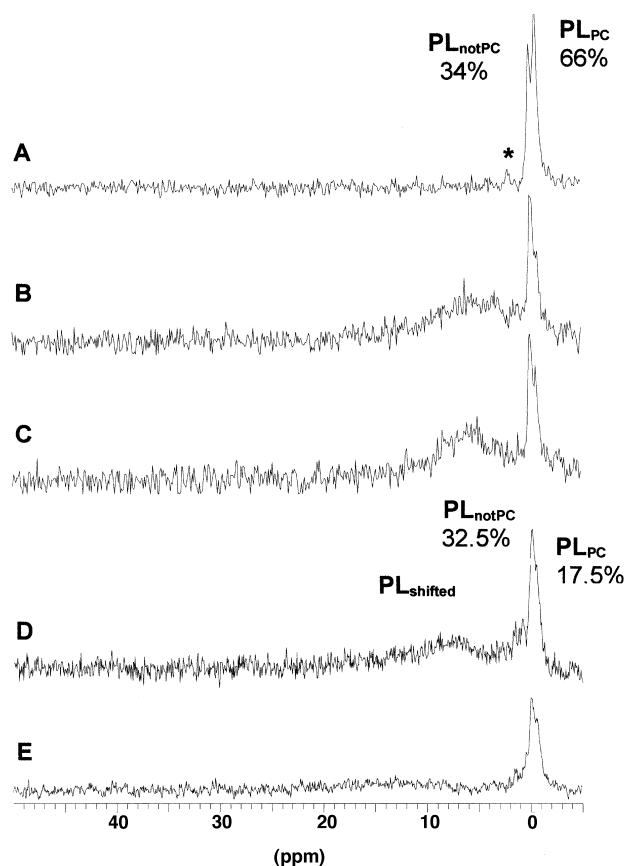


Fig. 5. 8 kHz MAS ^{31}P NMR spectra of sarcolemma vesicles (A) without PrCl_3 and (B–E) in the presence of 1, 2, 3 and 5 mM PrCl_3 performed at 202 MHz.

3.4. Effect of PrCl_3 on ^{31}P NMR spectra of sarcolemma vesicles

As previously observed [30], the ^{31}P NMR MAS spectrum of sarcolemma vesicles is made up of two major narrow resonances (Fig. 5A): the resonance at -0.63 ppm is from the phosphorus nuclei of phosphatidylcholine (PL_{PC}) and the resonance at -0.07 ppm is from the phosphorus nuclei of major PLs other than phosphatidylcholine (PL_{notPC}). The minor resonance at 2 ppm (* in Fig. 5A) is from inorganic phosphorus present in buffer A.

After the first addition of PrCl_3 to the vesicle exterior, a broad downfield resonance is observed amounting for about 50% of the total PLs. The two narrow resonances remain at the same chemical shifts, but their intensities are modified. Increasing concentrations of PrCl_3 lead to a progressive downfield shift of the broad resonance, whereas the relative intensities of all the PL resonances remain constant (Fig. 5B–E). The shifted signal ($\text{PL}_{\text{shifted}}$) corresponds to PLs located on

Table 1
Calculated compositions of PL_{PC} and PL_{notPC} for internal and external layers of the vesicle membrane (expressed as a percentage of total PLs)

	Internal layer	External layer ^a
PL_{PC}	17.5	48.5
PL_{notPC}	32.5	1.5

^a $(\text{PL})_{\text{external}} = (\text{PL})_{\text{without PrCl}_3} - (\text{PL})_{\text{internal}}$

the outer side of the vesicle membranes, which may be in contact with Pr^{3+} ions. By contrast, the unshifted signals represent the portion of PL_{PC} and PL_{notPC} located within the internal layer. For a full quantitative analysis, see below.

^{31}P NMR spectra obtained over three consecutive days following the addition of 5 mM PrCl_3 are identical to the initial spectrum (data not shown). Moreover, identical results are obtained for sarcolemma vesicles incubated with 5 mM PrCl_3 at 1, 2 and 3 days after the isolation procedure.

Comparing the broad-band ^{31}P NMR spectrum without PrCl_3 (Fig. 3A) with the broad-band ^{31}P NMR spectrum with PrCl_3 (Fig. 6A), we observe an additional very intense broad resonance at 16 ppm in the latter. This band accounts for about half of the PLs. Using the same strategy of assignment as for MAS spectra, this signal is assigned to PLs of the external layer in contact with Pr^{3+} ions. Assuming a mixed Lorentzian and Gaussian deconvolution for this symmetric band, the high-field resonance is well-fitted using a powder-like peak shape (Fig. 6). Proton decoupling has no effect on the peak shape of spectra acquired with PrCl_3 (Fig. 6).

Furthermore, the integrity of membrane vesicles at all PrCl_3 concentrations is demonstrated by the constant resonance level of inorganic phosphate. This confirms that these paramagnetic ions do not penetrate into the vesicles.

3.5. Trans-bilayer PL distribution in the vesicle membranes

In the absence of PrCl_3 in five identical experiments, the PL_{PC} and PL_{notPC} resonances represented 66 ± 4 and $34 \pm 4\%$ of the total PLs, respectively (Fig. 5A).

The quantitative analyses of $\text{PL}_{\text{shifted}}$, PL_{PC} and PL_{notPC} resonances in the presence of PrCl_3 are reported on the spectrum in Fig. 5D. The broad-shifted resonance represents

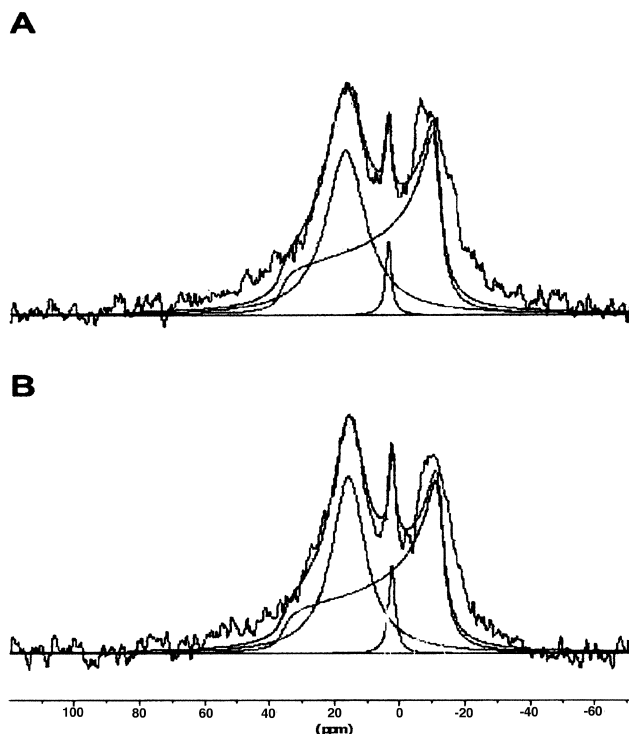


Fig. 6. (A) Experimental non-decoupled and (B) proton decoupled broad-band ^{31}P NMR spectrum of sarcolemma vesicles, performed at 202 MHz with 5 mM PrCl_3 , using the narrow line fits obtained with WinFit software (see text).

roughly 50% of the total intensity, while PL_{PC} and PL_{notPC} resonances in five identical experiments represent 35 ± 4 and $65 \pm 4\%$ of the unshifted resonances, respectively. Hence, knowing the proportion of PLs in the internal layer and assuming that they represented about 50% of total PLs, PL_{PC} and PL_{notPC} levels in the internal layer correspond to 17.5 and 32.5% of the total PLs. We can then calculate the PL_{notPC} and PL_{PC} composition of the external layer of the vesicle membrane (Table 1). It is clear that these two classes of PLs are distributed asymmetrically between the two layers of the vesicle membrane. The proportion of phosphatidylcholine is very high in the external layer, while the other PLs are preferentially located in the internal layer of the vesicle membrane.

3.6. T_1 longitudinal relaxation time measurements

The relaxation time T_1 measured on PL_{PC} and PL_{notPC} lines on samples without $PrCl_3$ are 1.00 ± 0.06 s and 0.96 ± 0.05 s in six identical experiments, respectively. T_1 on samples with $PrCl_3$ are found to be 0.97 ± 0.12 s and 1.15 ± 0.15 s for the unshifted PL_{PC} and PL_{notPC} lines in three identical experiments, respectively. These values are similar to those obtained on the same lines without $PrCl_3$.

4. Discussion and conclusion

In this study, we combine two methods – ^{31}P NMR spectroscopy and electron microscopy – to investigate the structural arrangement and dynamics of PLs in the isolated sarcolemma membrane of normal skeletal muscle.

We show, by immuno-labelling, that vesicle sarcolemma membranes maintain the natural orientation of in-vivo muscle cells, i.e. the internal layer of muscle cell membranes is found only inside the vesicle membranes, despite the long isolation procedure. This result gives great biological relevance to the NMR findings. We also show that the motions are quite similar in natural sarcolemma membrane compared with model membranes [33,35–37]. This is based on peak-shape simulations of broad-band spectra that yield information about slow motions (specifically, lateral diffusion) and on T_1 relaxation time measurements which provide more detailed information about rapid motions on short time scales.

By combining static and MAS ^{31}P NMR spectroscopy with lanthanide ions, we are able to achieve a simple and relatively accurate method for studying the trans-bilayer PL distribution without modifying the membrane. In the case of model membranes [16–18,21–23], our NMR results show that: (1) sarcolemma membranes are impermeable to Pr^{3+} ions because no spectral change is observed after incubation for 3 days, while the ratio of external to internal PLs remains constant. Furthermore, T_1 relaxation times of the internal PLs are not modified by the presence of Pr^{3+} ions; (2) at various $PrCl_3$ concentrations, the presence of a single progressively shifted resonance indicates a rapid exchange rate on the NMR time scale between the paramagnetic ions and the lipid head-groups of the external layer; (3) after sonication, all PLs are able to interact with Pr^{3+} ions since all phosphorus NMR signals are shifted downfield.

Brown and Seelig [20] observed a reversal in the sign of the CSA on addition of Eu^{3+} to liposomes, together with a large chemical shift. These authors suggested that a reorientation of the lipid head-groups could produce a reversal in the sign of

the CSA. In the present study, we recorded no such modification. Instead, a second large symmetrical peak appeared, strongly downfield-shifted and corresponding to about half of the total PLs. This broad symmetrical peak shape is due to the strong interaction between the electronic spin of the Pr^{3+} and the magnetic spin of the phosphorus nucleus, which dominates the interaction of its magnetic spin with the static magnetic field B_0 , i.e. the CSA. This strong interaction could not be averaged by MAS and the peak-width appeared roughly the same in the broad-band as in the MAS spectrum.

Using MAS ^{31}P NMR spectroscopy with $PrCl_3$, we were also able to distinguish internal from external PLs in the natural membrane and quantify the phosphatidylcholine distribution between the two layers. It appears that the sarcolemma PLs of skeletal muscle are distributed asymmetrically between the two layers and, as in other cell types, phosphatidylcholine is preferentially located in the external layer [5,6].

Previous studies on model membranes showed that lipids in SUVs are asymmetrically distributed due to packing constraints and electrostatic repulsion between charged lipids. However, the asymmetry tends to decrease as the vesicle size increases [14,38,39]. The diameter of the sarcolemma vesicles (≈ 250 nm) in our study corresponds to the minimum size that could be obtained without the physical constraints of sonication, filtration or freeze/thaw [33]. Therefore, at the molecular level, the bilayer in the vesicle membrane can be considered as flat [40]. Nevertheless, PLs are distributed asymmetrically, suggesting that another effect could play an important role in their distribution and preservation.

Among other mechanisms involved in the preservation of asymmetry, workers have suggested the action of peripheral or integral proteins [41,42]. Since the vesicle membrane is sealed *inside-in*, i.e. with dystrophin inside the vesicles, we could argue that this protein participates in the preservation of the trans-bilayer asymmetrical distribution of PLs as well as their natural curvature [43]. In support of this idea, a high affinity has already been described between dystrophin and anionic PLs [44]. Furthermore, it is known that dystrophin is lacking and the plasma membrane is profoundly modified in Duchenne muscular dystrophy [1,2]. In particular, the anchorage of integral proteins interacting with dystrophin does not take place. However, the PL structure in the sarcolemma of such pathological muscles has not yet been investigated. Studies currently in progress should provide important data supporting this hypothesis.

Acknowledgements: The authors wish to thank Pierre-Antoine Eliat, Roselyne Primault and Emmanuelle Guiot for their skilful technical assistance. Dr M.S.N. Carpenter corrected the English style. This work was supported by grants and fellowships for C.M. and M.T. from the Association Française contre les Myopathies.

References

- [1] Straub, V. and Campbell, K.P. (1997) *Curr. Opin. Neurol.* 10, 168–175.
- [2] Ozawa, E., Yasuko, Y. and Yoshida, M. (1999) *Mol. Cell Biochem.* 190, 143–151.
- [3] Bretscher, M.S. (1972) *Nature* 236, 11–12.
- [4] Verkleij, A.J., Zwaal, R.F., Roelofsen, B., Comfurius, P., Kasteleijn, D. and Van deenen, L.L.M. (1973) *Biochim. Biophys. Acta* 323, 178–193.
- [5] Rothman, E. (1977) *Sciences* 195, 743–753.
- [6] Devaux, P.F. (1991) *Biochemistry* 30, 1163–1173.

- [7] Musters, R.J.P., Otten, E., Bijvelt, J., Keijzer, J.J.H., Post, J.A., Op den Kamp, J.A.F. and Verkleij, A.J. (1993) *Circ. Res.* 73, 514–523.
- [8] Andree, H.A.M., Stuart, M.C.A., Hermens, W.T., Reuteling-sperger, C.P.M., Hemker, H.C., Frederik, P.M. and Willems, G.M. (1992) *J. Biol. Chem.* 267, 17907–17912.
- [9] Shukla, S.D. and Hanahan, D.J. (1982) *Arch. Biochem. Biophys.* 214, 335–341.
- [10] Bergelson, L.D. and Barsukov, L.I. (1977) *Science* 197, 224–230.
- [11] Op den Kamp, J.A.F. (1979) *Annu. Rev. Biochem.* 48, 47–71.
- [12] Zachowski, A. (1993) *Biochem. J.* 294, 1–14.
- [13] Bystrov, V.F., Dubrovina, N.I., Barsukov, L.I. and Bergelson, L.D. (1971) *Chem. Phys. Lipids* 6, 343–350.
- [14] Berden, J.A., Barker, R.W. and Radda, G.K. (1975) *Biochim. Biophys. Acta* 375, 186–208.
- [15] De Kruijff, B., Cullis, P. and Radda, G. (1975) *Biochim. Biophys. Acta* 406, 6–20.
- [16] Hauser, H., Phillips, M.C., Levine, B.A. and Williams, R.J.P. (1975) *Eur. J. Biochem.* 58, 133–144.
- [17] Nolden, P.W. and Ackermann, T. (1976) *Biophys. J.* 4, 297–304.
- [18] Haran, N. and Shporer, M. (1977) *Biochim. Biophys. Acta* 465, 11–18.
- [19] Hutton, W.C., Yeagle, P.L. and Martin, R.B. (1977) *Chem. Phys. Lipids* 19, 255–265.
- [20] Brown, M.F. and Seelig, J. (1977) *Nature* 269, 721–723.
- [21] Barsukov, L.I., Victorov, A.V., Vasilenko, I.A., Evstigneeva, R.P. and Bergelson, L.D. (1980) *Biochim. Biophys. Acta* 598, 153–168.
- [22] Nordlund, J.R., Schmidt, C.F. and Thompson, T.E. (1981) *Biochemistry* 20, 6415–6420.
- [23] Frölich, M., Brecht, V. and Peschka-Süss, R. (2001) *Chem. Phys. Lipids* 109, 103–112.
- [24] De Kruijff, B., Van den Besselaar, A.M.H.P., Van den Bosch, H. and Van Deenen, L.L.M. (1979) *Biochim. Biophys. Acta* 555, 181–192.
- [25] Oldfield, E., Bowers, J.L. and Forbes, J. (1987) *Biochemistry* 26, 6919–6923.
- [26] Forbes, J., Bowers, J., Shan, X., Moran, L., Oldfield, E. and Moscarello, M.A. (1988) *J. Chem. Soc. Faraday Trans. 1*, 3821–3849.
- [27] Forbes, J., Husted, C. and Oldfield, E. (1988) *J. Am. Chem. Soc.* 110, 1059–1065.
- [28] Pinheiro, T.J.T. and Watts, A. (1994) *Biochemistry* 33, 2459–2467.
- [29] Traïkia, M., Langlais, D.B., Cannarozzi, G.M. and Devaux, P.F. (1997) *J. Magn. Res.* 125, 140–144.
- [30] Moreau, C., Le Floch, M., Segalen, J., Leray, G., Metzinger, L., de Certaines, J.D. and Le Rumeur, E. (1999) *FEBS Lett.* 461, 258–262.
- [31] Beuron, F., Le Cahérec, F., Guillam, M.T., Cavalier, A., Garret, A., Tassan, J.P., Delamarche, C., Schultz, P., Mallouh, V., Rolland, J.P., Hubert, J.F., Gouranton, J. and Thomas, D. (1995) *J. Biol. Chem.* 270, 17414–17422.
- [32] Douliez, J.P., Bellocq, A.M. and Dufourc, E.J. (1994) *J. Chem. Phys.* 91, 874–880.
- [33] Traïkia, M., Warschawski, D.E., Recouvreur, M., Cartaud, J. and Devaux, P.F. (2000) *Eur. J. Biophys.* 29, 184–195.
- [34] Ohlendieck, K. (1996) *Eur. J. Cell Biol.* 69, 1–10.
- [35] Dufourc, E.J., Mayer, C., Stohrer, J., Althoff, G. and Kothe, G. (1992) *Biophys. J.* 61, 42–57.
- [36] Fenske, D.B. (1993) *Chem. Phys. Lipids* 64, 143–162.
- [37] Auger, M. (1997) *Biophys. Chem.* 68, 233–241.
- [38] Israelachvili, J., Mitchell, J. and Ninham, B. (1977) *Biochim. Biophys. Acta* 470, 185–201.
- [39] Roy, M.T., Gallardo, M. and Esterrich, J. (1997) *Bioconjug. Chem.* 8, 941–945.
- [40] Sackmann, E. (1994) *FEBS Lett.* 346, 3–16.
- [41] Haest, C.W.M. (1982) *Biochim. Biophys. Acta* 694, 331–352.
- [42] Diakowski, W., Prychidny, A., Swistak, M., Niuetybyc, M., Bialkowska, K., Szopa, J. and Sikorski, A.F. (1999) *Biochem. J.* 338, 83–90.
- [43] Devaux, P.F. (2000) *Biochimie* 82, 497–509.
- [44] DeWolf, C., McCauley, P., Sikorski, A.F., Winlove, C.P., Bailey, A.I., kahana, E., Pinder, J.C. and Gratzer, W.B. (1997) *Biophys. J.* 72, 2599–2604.